https://doi.org/10.5194/tc-2020-28
Preprint. Discussion started: 10 March 2020

The Cryosphere Discussions
Open Access
EGU

Exploring the impact of atmospheric forcing and basal boundary conditions on the simulation of the Antarctic ice sheet at the Last Glacial Maximum

Javier Blasco[1,2], Jorge Alvarez-Solas[1,2], Alexander Robinson[1,2,3], and Marisa Montoya[1,2]

[1]Departamento de Física de la Tierra y Astrofísica, Universidad Complutense de Madrid, Facultad de Ciencias Físicas, 28040 Madrid, Spain
[2]Instituto de Geociencias, Consejo Superior de Investigaciones Científicas-Universidad Complutense de Madrid, 28040 Madrid, Spain
[3]Potsdam Institute for Climate Impact Research, 14473 Potsdam, Germany

Correspondence to: J. Blasco (jablasco@ucm.es)

Abstract. Little is known about the distribution of ice in the Antarctic ice sheet (AIS) during the Last Glacial Maximum (LGM). Whereas marine and terrestrial geological data indicate that the grounded ice advanced to a position close to the continental-shelf break, the total ice volume is unclear. Glacial boundary conditions are potentially important sources of uncertainty, in particular basal friction and climatic boundary conditions. Basal friction exerts a strong control on the large-scale dynamics of the ice sheet and thus affects its size, and is not well constrained. Glacial climatic boundary conditions determine the net accumulation and ice temperature, and are also poorly known. Here we explore the effect of the uncertainty in both features on the total simulated ice storage of the AIS at the LGM. For this purpose we use a hybrid ice-sheet-shelf model that is forced with different basal-drag choices and glacial background climatic conditions obtained from the LGM ensemble climate simulations of the third phase of the Paleoclimate Modelling Intercomparison Project (PMIP3). For a wide range of plausible basal friction configurations, the simulated ice dynamics vary widely but all simulations produce fully extended ice sheets towards the continental-shelf break. More dynamically active ice sheets correspond to lower ice volumes, while they remain consistent with the available constraints on ice extent. Thus, this work points to the possibility of an AIS with very active ice streams during the LGM. In addition, we find that the surface boundary temperature field plays a crucial role in determining the ice extent through its effect on viscosity. For ice sheets of a similar extent and comparable dynamics, we find that the precipitation field determines the total AIS volume. However, precipitation is highly uncertain. Climatic fields simulated by climate models show more precipitation in coastal regions than a spatially uniform anomaly, which can lead to larger ice volumes. We strongly support using these paleoclimatic fields to simulate and study the LGM and potentially other time periods like the Last Interglacial. However, their accuracy must be assessed as well, as differences between climate model forcing lead to a range in the simulated ice volume and extension of about 6 m sea-level equivalent and one million km^2.

https://doi.org/10.5194/tc-2020-28
Preprint. Discussion started: 10 March 2020


The Cryosphere Discussions
Open Access
EGU

1 Introduction

Sea-level variations on long timescales are driven by the waxing and waning of large continental ice sheets. The characterisation of the sensitivity of ice sheets to past climate changes is fundamental to gaining insight into their underlying dynamics as well as their response to future climate change. In addition, understanding past sea-level changes is important for quantifying sea-level rise (Nicholls and Cazenave, 2010; Defrance et al., 2017; King and Harrington, 2018; Golledge et al., 2019; Robel et al., 2019) and for assessing the risk of crossing tipping points within the Earth System, such as the collapse of the West Antarctic Ice Sheet (Kopp et al., 2009; Sutter et al., 2016; Pattyn et al., 2018).

The Antarctic Ice Sheet (AIS), in particular, plays a fundamental role as it is the largest ice sheet on Earth and stores ca. 58 meters of sea-level equivalent (msle; Fretwell et al. (2013)). Due to its size it is potentially the largest contributor to future sea-level projections, but it is also the most uncertain (Collins et al., 2013). Assessing the AIS contribution to the total sea-level budget at different time periods has proven to be challenging. The Last Glacial Maximum (LGM, 21 ka BP) represents an ideal benchmark period since there is a large availability and variety of proxy data that, furthermore, indicate important AIS changes relative to present day (PD). Both, marine and terrestrial geological data, indicate that at the LGM, the AIS extended up to the continental-shelf break (Anderson et al., 2002, 2014; Hillenbrand et al., 2012, 2014; The RAISED Consortium, 2014; Mackintosh et al., 2014). However, its exact extent is not well constrained everywhere. Whereas its advance in the Amundsen region, the Bellingshausen Sea and the Antarctic Peninsula is well established, in the Ross Sea and the East Antarctic region it remains controversial (Stolldorf et al., 2012; The RAISED Consortium, 2014). Furthermore, the total AIS ice volume is even less well constrained (Simms et al. (2019) and references therein). Geological data furthermore do not provide direct information on past thickness and volume of ice sheets, which must hence be inferred. There have been several approaches to infer past ice-volume change of an individual ice sheet as the AIS. One approach is to use direct ice-sheet modelling to simulate the volume of the AIS at the LGM (e.g Huybrechts (2002); Whitehouse et al. (2012a); Golledge et al. (2012); Gomez et al. (2013); Maris et al. (2014); Briggs et al. (2014); Quiquet et al. (2018)). An alternative is to use Glacial Isostatic Adjustment (GIA) modelling, which describes the viscous response of the solid Earth to past changes in surface loading by ice and water (e.g. Ivins and James (2005); Bassett et al. (2007)). This approach has also been used in combination with direct ice-sheet modelling (e.g. Whitehouse et al. (2012b)) and/or by making use of constraints on ice-thickness from reconstructions based on exposure age dating, as well as satellite observations of current uplift (Whitehouse et al., 2012b; Ivins et al., 2013; Argus et al., 2014b). Whereas older studies estimated large sea-level contributions generally above 15 m (e.g. Nakada et al. (2000); Huybrechts (2002); Peltier and Fairbanks (2006); Philippon et al. (2006); Bassett et al. (2007)), more recent modelling studies and reconstructions have lowered these estimates to 7.5-13.5 m (Mackintosh et al., 2011; Whitehouse et al., 2012a; Golledge et al., 2012, 2014; Gomez et al., 2013; Argus et al., 2014b; Briggs et al., 2014; Maris et al., 2014; Sutter et al., 2019). Several factors have contributed to a decrease in the estimate of the LGM AIS volume. On one hand, the state of the art of ice-sheet modelling has considerably advanced in the last years, for example through the inclusion of more complex physics, increased spatial resolution and sub-grid scale grounding-line treatment (e.g. Goelzer et al. (2017); Pattyn (2018)). On the other hand, external processes, like the ice-ocean interaction or the GIA, are now treated with more accurate parameterisations and models

https://doi.org/10.5194/tc-2020-28
Preprint. Discussion started: 10 March 2020

(e.g., Reese et al. (2018); Whitehouse et al. (2019)). Nevertheless, the latest LGM AIS volume estimates still differ by more than 5 msle.

Given that ablation and basal melting were probably negligible at the LGM in the AIS, ice-sheet dynamics and accumulation must have been the two main factors controlling ice-mass gain during this period. The representation of ice dynamics in ice-sheet models is a key feature that can potentially lead to important discrepancies. Most ice-sheet models simulating the past long-term evolution of large-scale ice sheets are hybrid models that rely on the Shallow Ice Approximation (SIA) and the Shallow Shelf Approximation (SSA). Moreover, there is no universally accepted friction law, and basal friction is treated in different manners in ice-sheet models. Ritz et al. (2015) emphasize the importance of the basal friction, as it can favour the occurrence of the marine instability in future AIS projections. Generally, basal stress follows either a power-law formulation on the basal ice velocity (a special case being the Weertman (1957) friction law) or a Coulomb friction law (Schoof, 2005) with different power-law coefficients, a friction coefficient and potentially a regularization term. Ice-sheet models thus use friction formulations that can range from linear viscous and regularized Coulomb friction laws, typical of hard bedrock sliding (Larour et al., 2012; Pattyn et al., 2013; Joughin et al., 2019) to Coulomb-plastic deformation, characteristic of ice flow over a soft bedrock with filled cavities (Schoof, 2005, 2006; Nowicki et al., 2013). In the simplest cases a constant friction coefficient is prescribed over the whole domain (Golledge et al., 2012), but generally this parameter incorporates the dependency of basal friction on the effective pressure exerted by the ice, as well as on bedrock characteristics by making use of assumed till properties (Winkelmann et al., 2011; Albrecht et al., 2019; Sutter et al., 2019) or basal temperature conditions (Pattyn, 2017; Quiquet et al., 2018). The sensitivity of the simulated ice volume to these features is substantial. For instance, Briggs et al. (2013) obtained differences of more than 5 msle for an Antarctic LGM state depending only on the friction coefficients used for hard and soft beds. Some studies have attempted to overcome the uncertainty in basal friction by optimising the friction coefficient through inversion methods in order to obtain an accurate PD ice-sheet state (Morlighem et al., 2013; Le clec'h et al., 2019). However, these optimizations are based on a particular configuration of the PD state, and it is unclear whether they remain valid for glacial conditions. All in all, basal friction is poorly characterised, and the potential consequences of the associated uncertainty should be considered in ice-sheet modeling.

Glacial atmospheric boundary conditions over Antarctica are also far from being well constrained. It is clear from ice-core records and marine deep-sea sediment data that, at the continental scale, temperatures were lower than today and that the climate was drier (Frieler et al., 2015; Fudge et al., 2016). Typically, ice-sheet models use two approaches for simulating the atmospheric conditions at the LGM. On one hand, some studies prescribe a spatially-uniform temperature anomaly (generally between 8 K and 10 K below PD) and a uniform reduction in precipitation (generally by 40-50% compared to PD), as inferred from individual ice-core records (Huybrechts, 2002; Golledge et al., 2012; Whitehouse et al., 2012a; Gomez et al., 2013; Quiquet et al., 2018). However, this approach provides only a crude representation of glacial climate anomalies. In reality, even if ice cores show a similar temperature decrease, estimated precipitation changes are less homogeneous. Thus imposing a constant change over the whole domain will potentially misrepresent climatologies in localized areas (Frieler et al., 2015; Fudge et al., 2016). In addition, ice cores are extracted from domes and the recorded changes are not necessarily representative of coastal regions. Because the LGM is a cold state, with presumably no (or negligible) ablation and oceanic basal melt, the

https://doi.org/10.5194/tc-2020-28
Preprint. Discussion started: 10 March 2020

reduction of precipitation with respect to the PD should have an important impact on the size of the simulated ice sheet. In addition, because the temperature and/or precipitation anomalies are uniform, the PD pattern is imprinted on the LGM atmospheric forcing fields, and changes in atmospheric patterns are thus neglected.

Another commonly used method is to prescribe the LGM temperature and precipitation fields for the whole Antarctic domain from climate simulations (Briggs et al., 2013; Maris et al., 2014; Sutter et al., 2019). Output from simulations using a hierarchy of climate models has been used in the literature, from global general circulation models (GCMs) (Sutter et al., 2019), sometimes downscaled with regional models (Maris et al., 2014), to Earth System Models of Intermediate Complexity (EMICs) (Blasco et al., 2019). Briggs et al. (2013) went a step forward to investigate the effect of uncertainty in the climate forcing fields by assessing the effect of the inter-model variance through an empirical orthogonal function (EOF) analysis. However, some model outputs do not simulate the temperature anomalies correctly at specific sites where proxies are available, such as Vostok or Dome C. This may lead to an unrealistic configuration and thus it is necessary to evaluate the accuracy of model outputs (Cauquoin et al., 2015).

In this work we aim to assess the effects of the uncertainty in basal friction and climatic (in particular atmospheric) boundary conditions on the simulated LGM AIS. We focus on basal-drag choices which can lead to realistic LGM states. For these we then investigate the effect of different temperature and precipitation fields. To this end, we use a thermomechanical ice-sheet-shelf model forced with LGM background conditions. The atmospheric temperature and precipitation fields are obtained from the eleven GCMs participating in the Paleoclimate Modelling Intercomparison Project Phase III (PMIP3) as part of the Coupled Model Intercomparison Project Phase 5 (CMIP5, Taylor et al. (2012)). The article is structured as follows. First, we describe the ice-sheet-shelf model used and the experimental setup (Section 2). Then, we show the results obtained for different basal friction coefficients and atmospheric conditions (Section 3). Finally, the results are discussed (Section 4) and summarized in the conclusions (Section 5).

2 Methods and experimental setup

For this study we use the three-dimensional, hybrid, thermomechanical ice-sheet-shelf model Yelmo (Robinson et al., 2019). The model covers the whole Antarctic domain with 191x191 grid cells of 32km x 32km resolution and 21 layers in sigma-coordinates. The flow of the grounded ice is computed as the sum of the solutions of the Shallow Ice Approximation (SIA, Hutter (1983)) and the Shallow Shelf Approximation (SSA, MacAyeal (1989)). Sliding occurs only within the SSA solution, where the computed basal velocity is corrected with the corresponding basal friction. Ice shelves are solved within the SSA solution without basal drag. The initial topographic conditions (ice thickness, surface and bedrock elevation) are obtained from the RTopo-2 dataset (Schaffer et al., 2016). The internal ice temperature is calculated via the advection-diffusion equation.

Yelmo computes the total mass balance (MB) as a sum of the surface mass balance (SMB), the basal mass balance at the ice base and calving at the ice front. The SMB is obtained as a difference between the ice accumulation through precipitation and surface melting using the positive degree-day method (PDD; Reeh (1989)). Although there are more comprehensive methods that account for short-wave radiation for instance (Robinson et al., 2011), the PDD scheme is commonly used in ice models

https://doi.org/10.5194/tc-2020-28
Preprint. Discussion started: 10 March 2020

in the Antarctic domain, because ablation at these latitudes is limited (Winkelmann et al., 2011; Pollard and DeConto, 2012; Pattyn, 2017). Furthermore, in this particular study, the transient character of the AIS evolution is not simulated, as we focus on the LGM period. Thus, there is no need for explicitly accounting for the effects of changes in insolation on melting. Calving occurs when the ice-front thickness decreases below an imposed threshold (200 m in this study) and the upstream ice flux is not large enough to provide the necessary ice for maintaining the previous thickness (Peyaud et al., 2007). Present-day basal melting rates at the ice-shelf base and at the grounding line are obtained from Rignot et al. (2013) and extrapolated over all 27 basins identified by Zwally et al. (2012). Below grounded ice, the basal mass balance is determined through the heat equation as in Greve and Blatter (2009), where the geothermal heat flux field is obtained from Shapiro and Ritzwoller (2004). The glacial isostatic adjustment (GIA) is computed with the elastic lithosphere-relaxed asthenosphere (ELRA) method (Le Meur and Huybrechts, 1996), where the relaxation time of the asthenosphere is set to 3000 years.

Yelmo does not explicitly model the impact of ice anisotropy on the ice flow, so the classical "enhancement factor" are used as a tuning parameter (Ma et al., 2010; Pollard and DeConto, 2012; Maris et al., 2014; Albrecht et al., 2019). For this study we found realistic PD states for $\mathrm{E_{grounded}}$=1.0 and for ice shelves E_{floating}=0.7.

2.1 Basal-drag law

As mentioned above basal sliding is calculated within the SSA solution, which is a function of the basal stress. Yelmo computes the basal stress at the ice base ($\boldsymbol{\tau_b}$) through a linear viscous friction law. It depends on the basal ice velocity ($\mathbf{u_b}$), the effective ice pressure (N_{eff}) and a tunable friction coefficient (c_b):

$$\boldsymbol{\tau_b} = \beta \mathbf{u_b}, \tag{1}$$

and

$$\beta = c_b N_{\mathrm{eff}} \tag{2}$$

is the basal-drag coefficient, in [$\mathrm{kPa\ yr\ m^{-1}}$]. c_b, given in [$\mathrm{yr\ m^{-1}}$], is a coefficient that reflects the bedrock characteristics, and N_{eff} is the effective ice pressure, given in [kPa]. Here we have parameterized c_b as a function of the bedrock elevation, z_b (positive above sea level), analogous to previous work (e.g., Martin et al. (2011)):

$$c_b = \begin{cases} c_{\mathrm{max}} & \text{if } z_b \geq 0 \\ \max\left[c_{\mathrm{max}} \exp\left(-\frac{z_b}{z_0}\right), c_{\mathrm{min}} \right] & \text{if } z_b < 0 \end{cases} \tag{3}$$

Here, z_0 is an internal parameter that determines the bedrock e-folding depth over which the friction coefficient c_b decreases from a maximum value of c_{max} reached for bedrock elevations above sea level ($z_b \geq 0$) and a minimum threshold value c_{min}. For higher values of z_0 (i.e., lower absolute values of z_0), c_b falls more rapidly with depth. This parameterisation captures the phenomenon by which the occurrence of sliding (and its intensity) is favoured at low bedrock elevations and specifically within the marine sectors of ice sheets. It follows a similar approach as in Albrecht et al. (2019) and Martin et al. (2011), where the bedrock friction (in their case the “till friction angle”) depends on the bedrock elevation.

https://doi.org/10.5194/tc-2020-28
Preprint. Discussion started: 10 March 2020

The effective pressure is represented by the Leguy et al. (2014) formulation, under the assumption that the subglacial drainage system is hydrologically well connected to the ocean so that there is full support from the ocean wherever the ice-sheet base is below sea level. We thus assume that the exerted basal pressure at the land-ice interface depends on the difference between the overburden pressure and the basal water pressure (i.e. the distance from flotation as measured in ice thickness), hence:

$$N_{\text{eff}} = \rho_i g \left(H - H_f\right) \tag{4}$$

where ρ_i is the density of ice, g is gravity, H is the ice thickness and H_f is the flotation thickness, given by $H_f = \max\left[0, -\frac{\rho_w}{\rho_i} z_b\right]$, where ρ_w is the seawater density, respectively, and z_b is the bedrock elevation (positive above sea-level). In this way, far from the grounding line, $H_f = 0$ and $N_{\text{eff}} = \rho_i g H$, while at the grounding line, where $H = H_f$, $N_{\text{eff}} = 0$. This ensures continuity of $\boldsymbol{\tau_b}$ at the grounding line.

2.2 Climate forcing

To simulate the AIS at the LGM, Yelmo is run over 80 kyr with constant LGM conditions. The atmospheric forcing field is given by the following equation:

$$T^{atm}_{\text{LGM}} = T^{atm}_0 + \Delta T^{atm}_{\text{LGM-PD}} \tag{5}$$

where T^{atm}_0 is the PD temperature field at sea level obtained from RACMO2.3 forced by the ERA-Interim reanalysis data (Van Wessem et al., 2014) and $\Delta T^{atm}_{\text{LGM-PD}}$ is the LGM surface temperature anomaly relative to the PD. The monthly-mean temperature fields are obtained from each of the the eleven PMIP3 models, as well as by the ensemble mean (Fig. 1a). We apply a lapse rate correction that accounts for changes in elevations (0.008 $\mathrm{K\ m^{-1}}$ for annual temperatures and 0.0065 $\mathrm{K\ m^{-1}}$ for summer temperatures).

The LGM precipitation is calculated as

$$P_{\text{LGM}} = P_0 \delta P_{\text{LGM/PD}} \tag{6}$$

where P_0 is the PD monthly-mean precipitation obtained in the same way as the PD temperature and $\delta P_{\text{LGM/PD}}$ is the relative anomaly between the LGM and PD obtained from the PMIP3 ensemble. Figure 1b shows the resulting precipitation field, P_{LGM}, for the PMIP3 ensemble mean. Precipitation is corrected with local temperature anomalies through Clausius-Clapeyron scaling, which assumes more accumulation for warmer temperatures and therefore lower elevations. Note that precipitation is given in water equivalent and transformed into accumulation via changes in density (i.e. 1 $\mathrm{m\ yr^{-1}}$ water equivalent ca. 1.09 m ice). Basal-melting rates for floating ice shelves are set to zero in the LGM state.

https://doi.org/10.5194/tc-2020-28
Preprint. Discussion started: 10 March 2020


The Cryosphere Discussions

2.3 Experimental set-up of the sensitivity studies

Basal friction

To investigate the impact of changes in basal friction on the LGM AIS we assess the sensitivity to the friction in marine zones via the minimum friction allowed (c_{min}) and the elevation parameter (z_0) in Eq. 3 that controls how quickly friction decreases with depth. For this purpose we force Yelmo with a single reference climatic state obtained from the average anomaly of the PMIP3 ensemble for the LGM climate (Fig. 1) and a range of friction parameters. This range was determined in two steps. First, PD AIS simulations were carried out. Values of c_{max}= 200·10^{-5} yr m^{-1} were found to simulate the PD AIS in good agreement with observations in terms of grounded ice volume and grounding-line advance for the selected range of values of c_{min} = 1·10^{-5}, 3·10^{-5} and 5·10^{-5} yr m^{-1} and of z_0 = -100, -125, -150, -175 and -200 m (see Supplementary Information, Fig. S1, S2). The parameter range for the LGM AIS simulations was then selected under the criterion that the simulated volume of ice above flotation in the corresponding PD AIS simulation is within ±3.5 msle of that calculated from PD observations as in Schaffer et al. (2016) (see Supplementary Information, Figure S1).

Climatic fields

To understand the impact of changes in climatic forcing on the ice sheet, we fix the friction parameter values to a single, reference set of values (z_0 = -175 m and c_{min} = 1·10^{-5} yr m^{-1}) and analyze the AIS simulated at the LGM for the climatic forcing derived from each of the 11 models in the PMIP3 ensemble, using the aforementioned forcings for temperature (Eq. 5) and precipitation (Eq. 6). We focus on how the temperature and precipitation fields control the size and extent of the ice sheet. In all experiments the sea-level change estimates are computed with respect to the simulated PD state for the reference friction parameter values.

3 Results

3.1 Impact of basal friction

Here we present our LGM simulated AIS for different basal friction parameters. Ice volume is converted into a sea-level contribution by subtracting the floating portion and taking isostatic depression of the bedrock into account (Goelzer et al., 2019). Figure 2a shows how the simulated ice volume (in msle) varies with the mean basal-drag coefficient (β) of the marine zones for c_{min} = 1·10^{-5} yr m^{-1} (circles), 3·10^{-5} yr m^{-1} (crosses) and 5·10^{-5} yr m^{-1} (diamonds). A higher mean marine friction (associated with lower z_0 values) is found to result in a larger ice volume. Sea-level differences between a case with rapidly decreasing marine friction (e.g. z_0=-100 m; in red) and a case with more gradually decreasing friction (e.g. z_0=-200 m, in blue) are about 7 msle. This can be explained by the fact that a higher basal friction slows the basal velocity and hence the ice flow, translating into thicker ice. Faster sliding in the deepest areas (lowest c_{min} values) also contributes to reduce the ice volume, but only by about 2 msle for the range of parameters explored. We do not identify a clear dependency of the simulated

https://doi.org/10.5194/tc-2020-28
Preprint. Discussion started: 10 March 2020


The Cryosphere Discussions

grounded area on the marine basal friction exerted, as the grounding-line position is similar in all cases (Fig. 2b). Our results fit well within the range of previous studies both in terms of simulated msle (Simms et al. (2019) and references therein) and reconstructions of ice extension from ICE-6G (Argus et al., 2014a; Peltier et al., 2015, 2018), The RAISED Consortium (2014) and the ANU reconstruction (Lambeck and Johnston, 1998; Lambeck and Chappell, 2001; Lambeck et al., 2002, 2003). Note that in order to avoid biases due to Yelmo's coarse spatial resolution, these extensions were computed using the ice-sheet margins of each of the reconstructions at Yelmo's spatial resolution. The three lowest bound simulations correspond to cases for which the corresponding PD AIS ice volume deviates from PD observations by more than 3.5 msle (see SI, Fig. S1, S2).

The simulated surface velocity pattern shows a distribution with low values near the summit and increasing values towards the margins (Fig. 3). Our friction parameterisation reproduces the fact that ice streams become faster on topographic lows with the Amery, Wilkes and Victorias Land showing active ice streams of more than 50 $\mathrm{m\ yr^{-1}}$ (Fig. 3a,b). The WAIS, due to its marine character, is also a very active sector. Ice volume differences between a slowly decreasing friction (z_0=-200 m) and a more rapidly decreasing friction (z_0=-150 m) primarily originate in the WAIS and the coastal marine regions of the EAIS and its surroundings (Fig. 3c), and are the result of higher basal velocities with lower friction values (Fig. 3d) leading to thinner ice.

Subtle differences are found when comparing the extension of grounded ice in our simulated AIS with previous reconstructions (Fig. 4); given the lack of sensitivity of the AIS extension to the friction coefficients explored here, the results are shown only for one set of parameters, c_{min}= $1{\cdot}10^{-5}$ $\mathrm{yr\ m^{-1}}$ and z_0=-175 m, an intermediate case between the high and low friction values previously discussed (hereafter our reference run). Our simulated grounded area (thick black line) covers almost 16 million $\mathrm{km^2}$ of the 17 million $\mathrm{km^2}$ of the continental-shelf break (i.e. defined by the contour z_b=-2000 m; grey shaded area). Our simulated extension stands between the ICE-6G model (green line in Fig. 4) and the RAISED Consortium (red line) and the ANU (blue line) model. The largest discrepancies between models occur on the Ross shelf. Whereas ANU and RAISED estimate an advance close to the continental-shelf break, ICE-6G is more retreated, while our results support a nearly complete advance.

3.2 Impact of climatic forcing

Here we present the simulated LGM AIS of each individual PMIP3 model for the reference friction parameters (Fig. 5). The simulated ice-volume anomaly ranges from 7.8 msle to 14.0 msle (Fig. 6), a difference of 6.2 msle. The total ice extension ranges from 14.6 million $\mathrm{km^2}$ to 15.8 million $\mathrm{km^2}$, a difference of 1.2 million $\mathrm{km^2}$. Thus, while the spread in ice volume is somewhat smaller than found when investigating the sensitivity to friction, the spread in extension is significantly larger.

Because the underlying dynamics in Yelmo are the same in all cases, the differences in size and extension can only be explained by differences in the climatic fields. To determine the causes underlying these differences, we investigate the sensitivity of the ice thickness and extension to the climatic fields used to force the ice-sheet model (Fig. 7). We find that higher accumulation results in a thicker ice sheet (Fig. 7a), but has no appreciable effect on the ice extension (Fig. 7b). For model climatologies for which the LGM ice sheet extends close to the continental-shelf break (an extension of around 15.5 million $\mathrm{km^2}$, see Fig 7d), the AIS ice volume increases with increasing accumulation (Fig. 7c). However, there are four climate models

https://doi.org/10.5194/tc-2020-28
Preprint. Discussion started: 10 March 2020

(CNRM-CM5, GISS-E2-R-150, GISS-E2-R-151, FGOALS-g2) that despite having higher accumulation on average than the ensemble mean, do not allow the ice sheet to advance as much as the other models, leading in all cases to extensions below 15 million km^2 (Fig. 7b). Therefore, the simulated AIS volume is smaller for these less advanced ice sheets, despite the relatively high accumulation rates imposed. For all the others, for which extension is around 15.5 million km^2, the AIS ice volume clearly increases with increasing accumulation (Fig 7c).

Further inspection allows us to identify the atmospheric temperature close to the grounding line (Fig 7d) as a critical factor in determining how far the AIS advances. Whereas low temperatures present similar ice extension, as it becomes warmer the ice sheet is more retreated. Given the low temperature values, ablation can be generally discarded as the source of this behaviour (SI Fig. S3; there is, however, one exception, as discussed below), so we turn our attention to ice viscosity. A necessary condition for marine-based ice sheets to advance is that the ice thickness at the grounding line overcomes the flotation criterion as sustained through accumulation and/or by inland ice flow. This condition is fulfilled when the ocean depth (z_b) is shallower than $\sim 90\%$ of the ice thickness. Warmer ice temperatures lower the ice viscosity (Fig. 7e) and prevent the grounding-line to thicken, as a consequence of enhanced ice flow, and advance towards more depressed bedrock zones. Therefore, simulations with lower ice viscosity as GISS-E2-R-150, GISS-E2-R-151 and FGOALS-g2 do not fully advance in the Ross shelf, Pine Island or the Amery (Fig. 5,6).

Finally, CNRM-CM5 is a particular case which does not fulfil any of our proposed hypotheses. Viscosity describes the fluidity of a material, therefore warmer temperatures enhance ice flow. Thus, following the same reasoning as before, one would expect a low viscosity as a consequence of a warmer ice column for CNRM-CM5, which is not the case (Fig. 7e). This model expands fully at the Ross shelf and Antarctic Peninsula zone, but the Ronne shelf is far from the grounding-line and the Amery shelf is even more retreated than PD (Fig. 5). The ice sheet does not advance in these regions due to the presence of abnormal ablation, which impedes the ice expansion (see SI, Fig. S3). We argue that the unexpected large viscosity is a consequence of two competing effects. The fully advanced regions, as the Ross basin, contribute to a rather low ice temperature and hence a high viscosity. On the other hand, the ablation zones such as the Ronne and Amery basin, have warmer ice temperatures which conclude into low viscosity. Therefore Fig. 7e shows that CNRM-CM5 has on average a warm ice column and a high viscosity. A similar reasoning can be applied to Figure 7a where the mean ice thickness is low despite its high accumulation.

In summary, we find that the choice of the boundary climate is crucial for the simulated LGM ice sheet. On one hand, the atmospheric temperatures near the coastal regions control the ice extension through viscosity. If the viscosity is too low, then the ice flows too fast, preventing the necessary thickening. Particularly, if the bedrock is too deep, the ice sheet's expansion will be hampered. Secondly, if the ice sheet extends close to the continental-shelf break, then the accumulation pattern will determine the total amount of ice volume. We find that for similarly extended ice sheets (IPSL-CM5A-LR and MRI-CGCM3), the sea-level difference due to accumulation differences is about 3.5 msle.

Spatially homogeneous approach

Applying a simple scheme that lowers the ice accumulation and surface temperature homogeneously over the whole domain is a common and valid approach at first order, because during the LGM, at continental scale, a colder and drier climate is

https://doi.org/10.5194/tc-2020-28
Preprint. Discussion started: 10 March 2020

expected (Huybrechts, 2002; Golledge et al., 2012; Whitehouse et al., 2012a; Gomez et al., 2013; Quiquet et al., 2018). We thus tested a spatially homogeneous scaling (hereafter, the homogeneous method) for comparison. All simulations simulated realistic SLE and ice extensions during the LGM for the same friction coefficients. In overall, consistently lower ice volumes as well as reduced ice extensions are simulated with the homogeneous method (Fig. S4). Again, because the ice dynamics are the same, this difference can only be explained by the climatic forcing. Moreover, because temperatures are not sufficiently high to produce ablation it points to ice accumulation differences. Fig. 8c illustrates the ice thickness difference between the two methods for a similar ice extension (Fig. 8a,b). The anomaly shows that the main source of this difference in ice volume and extension comes from the WAIS. The Antarctic Peninsula in particular shows a high positive thickness anomaly for the average PMIP3 climatic fields relative to the homogeneous case because the grounding-line does not advance there in the latter case. In the EAIS, the anomalies are not so pronounced, however inland ice is slightly thinner, whereas closer to the coast it is thicker. This anomaly pattern can be explained by the difference between the accumulation fields (Fig. 8d). The spatially homogeneous method accumulates more ice inland and and leads to a reduced accumulation towards the continental-shelf break, especially at the Ross shelf, Pine Island and the Antarctic Peninsula. Because ice cores are generally extracted from dome regions with colder conditions, it is expected that precipitation and air temperatures near the coast are underestimated by the homogeneous approach.

4 Discussion

4.1 Basal dragging law

Even at present-day it is difficult to estimate bed properties like basal temperature or ice velocities, which could improve our understanding of basal friction. Therefore, estimating bed properties at the LGM, where the total ice volume and extension is not fully constrained, adds a degree of difficulty. We covered a range of friction values which lead to realistic LGM and PD configurations. The simulated sea-level differences were about 7 msle between the extreme cases (Fig. 2). We found that the choice of different bedrock frictions has an impact on ice-stream activity in marine-based regions. For example, an AIS that extends up to the continental-shelf break, but with a relatively low volume increase, can be achieved through a very dynamically active ice sheet. In that case, marine regions, and more specifically the WAIS, have the potential to maintain fast ice streams at the LGM and still agree with PD observations.

The choice of a given and unique friction law for the whole AIS is still somewhat arbitrary and unconstrained. We focused on a linear viscous friction law commonly used in other studies (Morlighem et al., 2013; Quiquet et al., 2018; Alvarez-Solas et al., 2019). We are aware that other types of friction laws could have been tested, such as a regularized Coulomb law (Joughin et al., 2019) or a Coulomb-plastic behaviour (Nowicki et al., 2013), typically for ice flowing over a bedrock filled with cavities. However, the importance of saturated tills is specially determinant for transient simulations with a retreating grounding line. Given the large uncertainty we quantified for only one friction formulation, we expect that this range would increase further considering additional formulations.

https://doi.org/10.5194/tc-2020-28
Preprint. Discussion started: 10 March 2020

4.2 Sea-level and ice extent uncertainty

For our reference friction parameters we used the individual climate simulations of the participating PMIP3 groups as surface boundary forcing. The sea-level difference between the models was about 6.2 msle. The lowest sea-level contribution was 7.8 msle (CNRM-CM5) and the largest 14.0 msle (IPSL-CM5A-LR). These sea-level estimates were inside the range of other studies and reconstructions. From this point of view, we were not able to discard any specific model field. Nonetheless, it seems unrealistic that air temperatures were high enough to produce ablation during the LGM as seen in CNRM-CM5.

The simulated ice extension is determined through air temperatures. Warmer temperatures lower the ice viscosity. Due to the marine character of the AIS, a lower viscosity enhances ice flow leading to thin ice in regions where the bedrock is too deep, which prevents a complete advance towards the continental-shelf break. Forcing from the models GISS-E2-R-150 and GISS-E2-R-151 for instance do not allow a full advance in the Ross shelf, resembling the ICE-6G reconstruction (Fig. 4). Similarly, with FGOALS-g2 the advance into the Pine Island region or the Amery shelf advance is impeded (Fig. 5). On the other hand, if temperatures are sufficiently cold, less than -20ºC or so, then the ice fully advances as in the ANU reconstruction (Fig. 4). The RAISED Consortium has a similar extension, but presents two large ice shelves at the margins of the Ronne shelf, which we are not able to simulate. Again, the simulated ice extensions were inside the range of the reconstructions, and we could not exclude any case. But we found that in addition to the precipitation field, temperature fields play a crucial role as they have the potential to accelerate the ice by lowering the viscosity and determine the total grounded ice area, which in turn affects the grounded ice volume.

Of course there are several sources which could impact AIS volume estimates, aside from the climatology and basal friction. A change in bedrock depth, for instance, has profound implications on the simulated AIS, as it does not only change the local sea level, but it can also facilitate (or impede) the ice advance and retreat (Philippon et al., 2006). Here we used a simple parameterization that accounts for the elasticity of the lithosphere and a non-local response caused by lateral shift (Le Meur and Huybrechts, 1996). This formulation does not capture differences in the mantle viscosity as it applies the same spatially homogeneous time response. Nonetheless, the Antarctic bedrock is a complex component with different rheological properties. The WAIS for instance is a low-viscosity region where the bedrock deformation happens on a shorter timescale (Whitehouse, 2018; Whitehouse et al., 2019). The next generation of ice-sheet models coupled to GIA models may produce more realistic bedrock responses and hence help to improve the sea-level budget at the LGM. This can be helpful for instance to constrain the phase space of friction parameters.

4.3 Forcing methods

Overall, a homogeneous anomaly relative to present day simulates a lower ice volume as a consequence of low accumulation near the ice-sheet margins (Fig. 8b). This indicates that the AIS could have stored more ice at the LGM than estimated by studies applying such a scheme. As opposed to a spatially homogeneous method, GCM outputs are capable of representing local atmospheric effects, such as atmospheric circulation changes or localized precipitation structures. Thus, the latest ice-sheet models have begun to be forced by more detailed and arguably more realistic climatic fields (Briggs et al., 2013; Maris

https://doi.org/10.5194/tc-2020-28
Preprint. Discussion started: 10 March 2020

et al., 2014; Sutter et al., 2019). Nevertheless we have shown here that the spread of the simulated ice volume and ice extension for different climatic outputs can be equal to or larger than that resulting from different basal-dragging choices. The PMIP3 LGM climatologies are built with a prescribed ice extension and surface elevation (Abe-Ouchi et al., 2015). It is clear then, that by construction, ice models should be driven towards these particular configurations. Nonetheless GCM models may exhibit biases in the temperatures and precipitation in localized regions. A way to potentially test the plausibility of the employed climatic fields is to compare with ice proxies. We strongly recommend that paleo ice-sheet simulations should be performed with GCM outputs, as they capture more complex processes than a spatially homogeneous method, but the choice of the climatic fields has to be consistent with reconstructions. In the future with PMIP4 results, more accurate climatic fields are expected.

5 Conclusions

The ice dynamics and the boundary climatology are two essential building blocks for the simulation of an Antarctic LGM state. Here we studied the uncertainty in LGM ice volume associated with these two factors, by investigating the effect of the representation of basal friction and of the atmospheric forcing, respectively, in simulations. First, we tested a range of potential basal friction values of marine zones which simulated plausible LGM states. We found that for a simple linear friction law lower (larger) friction values enhance (diminish) the ice dynamics of marine zones and result in ice sheet configurations with less (more) ice volume, but still similar grounded ice extension. This led to several potential configurations of the AIS with a sea-level difference with respect to today in the range of 11.2 msle and 17.5 msle and with a total ice extension in the range of 15 to 16 million km^2. Then, for a particular friction configuration within the estimates of ice volume and extension, we studied the individual sea-level contribution from simulations driven by LGM climates provided by the eleven PMIP3 participating groups. We found ice volume anomalies ranging from 7.8-14.0 msle and extensions of 14.6 to 15.8 million km^2. Imposing the PMIP3 fields, whose climate simulations include dynamic adjustment to the LGM boundary conditions, translate into higher precipitation rates along the Antarctic coast, hence leading to a larger simulated ice volume compared to using a homogeneous anomaly method. The grounding-line advance is strongly determined by the atmospheric temperatures as well. Higher temperatures enhance ice flow reducing the ice viscosity. Because of the marine character of the AIS, relatively high temperatures near the coast can prevent ice expansion. Thus, along with improved knowledge of basal conditions, constraining broader possible climatic changes during the LGM is imperative to be able to reduce uncertainty in the AIS volume estimates for this time period.

Code and data availability

Yelmo is maintained as a git repository hosted at https://github.com/palma-ice/yelmo under the licence GPL-3.0. Model documentation can be found at https://palma-ice.github.io/yelmo-docs/. The results used in this paper are archived on Zenodo (http://doi.org/10.5281/zenodo.3701258).

https://doi.org/10.5194/tc-2020-28
Preprint. Discussion started: 10 March 2020

Author contributions. JB carried out the simulations, analyzed the results and wrote the paper. All other authors contributed to designing the simulations, analyzing the results and writing the paper.

Competing interests. The authors declare that they have no conflict of interest.

Acknowledgements. This project is TiPES contribution #8: This project has received funding from the European Union's Horizon 2020 research and innovation programme under grant agreement No 820970. This research has also been supported by the Spanish Ministry of Science and Innovation project RIMA (grant agreement No CGL2017-85975-R). Alexander Robinson was funded by the Ramón y Cajal Programme of the Spanish Ministry for Science, Innovation and Universities (grant agreement No RYC-2016-20587). Simulations were performed in EOLO, the HPC of Climate Change of the International Campus of Excellence of Moncloa, funded by MECD and MICINN. We thank I. Tabone for comments and helpful discussions.

https://doi.org/10.5194/tc-2020-28
Preprint. Discussion started: 10 March 2020

References

Abe-Ouchi, A., Saito, F., Kageyama, M., Braconnot, P., Harrison, S. P., Lambeck, K., Otto-Bliesner, B. L., Peltier, W., Tarasov, L., Peterschmitt, J.-Y., and Takahashi, K.: Ice-sheet configuration in the CMIP5/PMIP3 Last Glacial Maximum experiments, GMD, 8, 3621–3637, doi:10.5194/gmd-8-3621-2015, 2015.

Albrecht, T., Winkelmann, R., and Levermann, A.: Glacial cycles simulation of the Antarctic Ice Sheet with PISM – Part 1: Boundary conditions and climatic forcing (in review), The Cryosphere Discussion, doi:10.5194/tc-2019-71, 2019.

Alvarez-Solas, J., Banderas, R., Robinson, A., and Montoya, M.: Ocean-driven millennial-scale variability of the Eurasian ice sheet during the last glacial period simulated with a hybrid ice-sheet–shelf model, Climate of the Past, 15, 957–979, doi:10.5194/cp-15-957-2019, 2019.

Anderson, J. B., Shipp, S. S., Lowe, A. L., Wellner, J. S., and Mosola, A. B.: The Antarctic Ice Sheet during the Last Glacial Maximum and its subsequent retreat history: a review, Quaternary Science Reviews, 21, 49–70, doi:10.1016/S0277-3791(01)00083-X, 2002.

Anderson, J. B., Conway, H., Bart, P. J., Witus, A. E., Greenwood, S. L., McKay, R. M., Hall, B. L., Ackert, R. P., Licht, K., Jakobsson, M., and Stone, J.: Ross Sea paleo-ice sheet drainage and deglacial history during and since the LGM, Quaternary Science Reviews, 100, 31–54, doi:10.1016/j.quascirev.2013.08.020, 2014.

Argus, D., Peltier, W., Drummond, R., and Moore, A.: The Antarctica component of postglacial rebound model ICE-6G_C (VM5a) based on GPS positioning, exposure age dating of ice thicknesses, and relative sea level histories., Geophys. J. Int., 198, 537–563, doi:10.1093/gji/ggu140, 2014a.

Argus, D. F., Peltier, W., Drummond, R., and Moore, A. W.: The Antarctica component of postglacial rebound model ICE-6G_C (VM5a) based on GPS positioning, exposure age dating of ice thicknesses, and relative sea level histories, Geophysical Journal International, 198, 537–563, doi:10.1093/gji/ggu140, 2014b.

Bassett, S., Milne, G., Bentley, M., and Huybrechts, P.: Modelling Antarctic sea-level data to explore the possibility of a dominant Antarctic contribution to meltwater pulse IA, Quaternary Science Reviews, 26, 2113–2127, doi:10.1016/j.quascirev.2007.06.011, 2007.

Blasco, J., Tabone, I., Alvarez-Solas, J., Robinson, A., and Montoya, M.: The Antarctic Ice Sheet response to glacial millennial-scale variability, Climate of the Past, 15, 121–133, doi:10.5194/cp-15-121-2019, 2019.

Briggs, R., Pollard, D., and Tarasov, L.: A glacial systems model configured for large ensemble analysis of Antarctic deglaciation, The Cryosphere, 7, 1949–1970, doi:10.5194/tc-7-1949-2013, 2013.

Briggs, R. D., Pollard, D., and Tarasov, L.: A data-constrained large ensemble analysis of Antarctic evolution since the Eemian, Quaternary Science Reviews, 103, 91–115, doi:10.1016/j.quascirev.2014.09.003, 2014.

Cauquoin, A., Landais, A., Raisbeck, G., Jouzel, J., Bazin, L., Kageyama, M., Peterschmitt, J.-Y., Werner, M., Bard, E., and ASTER Team: Comparing past accumulation rate reconstructions in East Antarctic ice cores using 10Be, water isotopes and CMIP5-PMIP3 models, Climate of the Past, 11, 355–367, doi:10.5194/cp-11-355-2015, 2015.

Collins, M., Knutti, R., Arblaster, J., Dufresne, J., Fichefet, T., Friedlingstein, P., Gao, X., Gutowski, W., Johns, T., Krinner, G., Shongwe, M., Tebaldi, C., Weaver, A., and Wehner, M.: Long-term Climate Change: Projections, Commitments and Irreversibility., in: Climate Change 2013: The Physical Science Basis. Contribution of Working Group I to the Fifth Assessment Report of the Intergovernmental Panel on Climate Change [Stocker, T.F., D. Qin, G.-K. Plattner, M. Tignor, S.K. Allen, J. Boschung, A. Nauels, Y. Xia, V. Bex and P.M. Midgley (eds.)]., Cambridge University Press, 2013.

https://doi.org/10.5194/tc-2020-28
Preprint. Discussion started: 10 March 2020

Defrance, D., Ramstein, G., Charbit, S., Vrac, M., Famien, A. M., Sultan, B., Swingedouw, D., Dumas, C., Gemenne, F., Alvarez-Solas, J., and Vanderlinden, J.-P.: Consequences of rapid ice sheet melting on the Sahelian population vulnerability, Proceedings of the National Academy of Sciences, 114, 6533–6538, doi:10.1073/pnas.1619358114, 2017.

Fretwell, P., Pritchard, H. D., Vaughan, D. G., Bamber, J., Barrand, N., Bell, R., Bianchi, C., Bingham, R., Blankenship, D., Casassa, G., Catania, G., Callens, D., Conway, H., Cook, A. J., Corr, H. F. J., Damaske, D., Damm, V., Ferraccioli, F., Forsberg, R., Fujita, S., Gim, Y., Gogineni, P., Griggs, J. A., Hindmarsh, R. C. A., Holmlund, P., Holt, J. W., Jacobel, R. W., Jenkins, A., Jokat, W., Jordan, T., King, E. C., Kohler, J., Krabill, W., Riger-Kusk, M., Langley, K. A., Leitchenkov, G., Leuschen, C., Luyendyk, B. P., Matsuoka, K., Mouginot, J., Nitsche, F. O., Nogi, Y., Nost, O. A., Popov, S. V., Rignot, E., Rippin, D. M., Rivera, A., Roberts, J., Ross, N., Siegert, M. J., Smith, A. M., Steinhage, D., Studinger, M., Sun, B., Tinto, B. K., Welch, B. C., Wilson, D., Young, D. A., Xiangbin, C., , and Zirizzotti, A.: Bedmap2: improved ice bed, surface and thickness datasets for Antarctica, The Cryosphere, 7, doi:10.5194/tc-7-375-2013, 2013.

Frieler, K., Clark, P. U., He, F., Buizert, C., Reese, R., Ligtenberg, S. R., Van Den Broeke, M. R., Winkelmann, R., and Levermann, A.: Consistent evidence of increasing Antarctic accumulation with warming, Nature Climate Change, 5, 348, doi:10.1038/nclimate2574, 2015.

Fudge, T., Markle, B. R., Cuffey, K. M., Buizert, C., Taylor, K. C., Steig, E. J., Waddington, E. D., Conway, H., and Koutnik, M.: Variable relationship between accumulation and temperature in West Antarctica for the past 31,000 years, Geophysical Research Letters, 43, 3795–3803, doi:10.1002/2016GL068356, 2016.

Goelzer, H., Robinson, A., Seroussi, H., and Van De Wal, R. S.: Recent progress in Greenland ice sheet modelling, Current climate change reports, 3, 291–302, doi:10.1007/s40641-017-0073-y, 2017.

Goelzer, H., Coulon, V., Pattyn, F., de Boer, B., and Van De Wal, R. S.: Brief communication: On calculating the sea-level contribution in marine ice-sheet models, The Cryosphere Discussions, doi:10.5194/tc-2019-185, 2019.

Golledge, N., Menviel, L., Carter, L., Fogwill, C., England, M., Cortese, G., and Levy, R.: Antarctic contribution to meltwater pulse 1A from reduced Southern Ocean overturning, Nature Communications, 5, 5107, doi:10.1038/ncomms6107, 2014.

Golledge, N. R., Fogwill, C. J., Mackintosh, A. N., and Buckley, K. M.: Dynamics of the last glacial maximum Antarctic ice-sheet and its response to ocean forcing, Proceedings of the National Academy of Sciences, 109, 16 052–16 056, doi:10.1073/pnas.1205385109, 2012.

Golledge, N. R., Keller, E. D., Gomez, N., Naughten, K. A., Bernales, J., Trusel, L. D., and Edwards, T. L.: Global environmental consequences of twenty-first-century ice-sheet melt, Nature, 566, 65, doi:10.1038/s41586-019-0889-9, 2019.

Gomez, N., Pollard, D., and Mitrovica, J. X.: A 3-D coupled ice sheet–sea level model applied to Antarctica through the last 40 ky, Earth and Planetary Science Letters, 384, 88–99, doi:10.1016/j.epsl.2013.09.042, 2013.

Greve, R. and Blatter, H.: Dynamics of ice sheets and glaciers, 2009.

Hillenbrand, C.-D., Melles, M., Kuhn, G., and Larter, R. D.: Marine geological constraints for the grounding-line position of the Antarctic Ice Sheet on the southern Weddell Sea shelf at the Last Glacial Maximum, Quaternary Science Reviews, 32, 25–47, doi:10.1016/j.quascirev.2011.11.017, 2012.

Hillenbrand, C.-D., Bentley, M. J., Stolldorf, T. D., Hein, A. S., Kuhn, G., Graham, A. G., Fogwill, C. J., Kristoffersen, Y., Smith, J. A., Anderson, J. B., Larter, R. D., Melles, M., Hodgson, D. A., Mulvaney, R., and Sugden, D. E.: Reconstruction of changes in the Weddell Sea sector of the Antarctic Ice Sheet since the Last Glacial Maximum, Quaternary Science Reviews, 100, 111–136, doi:10.1016/j.quascirev.2013.07.020, 2014.

Hutter, K.: Theoretical glaciology; material science of ice and the mechanics of glaciers and ice sheets, D. Reidel Publishing Co./Tokyo, Terra Scintific Publishing Co, 1983.

https://doi.org/10.5194/tc-2020-28
Preprint. Discussion started: 10 March 2020

Huybrechts, P.: Sea-level changes at the LGM from ice-dynamic reconstructions of the Greenland and Antarctic ice sheets during the glacial cycles, Quaternary Science Reviews, 21, 203–231, doi:10.1016/S0277-3791(01)00082-8, 2002.

Ivins, E. R. and James, T. S.: Antarctic glacial isostatic adjustment: a new assessment, Antarctic Science, 17, 541–553, doi:10.1017/S0954102005002968, 2005.

Ivins, E. R., James, T. S., Wahr, J., O. Schrama, E. J., Landerer, F. W., and Simon, K. M.: Antarctic contribution to sea level rise observed by GRACE with improved GIA correction, Journal of Geophysical Research: Solid Earth, 118, 3126–3141, doi:10.1002/jgrb.50208, 2013.

Joughin, I., Smith, B. E., and Schoof, C. G.: Regularized Coulomb friction laws for ice sheet sliding: Application to Pine Island Glacier, Antarctica, Geophysical Research Letters, 46, 4764–4771, doi:10.1029/2019GL082526, 2019.

King, A. D. and Harrington, L. J.: The inequality of climate change from 1.5 to 2 C of global warming, Geophysical Research Letters, 45, 5030–5033, doi:10.1029/2018GL078430, 2018.

Kopp, R. E., Simons, F. J., Mitrovica, J. X., Maloof, A. C., and Oppenheimer, M.: Probabilistic assessment of sea level during the last interglacial stage, Nature, 462, 863, doi:10.1038/nature08686, 2009.

Lambeck, K. and Chappell, J.: Sea level change through the last glacial cycle, Science, 292, 679–686, doi:10.1126/science.1059549, 2001.

Lambeck, K. and Johnston, P.: The viscosity of the mantle: Evidence from analyses of glacial rebound phenomena, The Earth's Mantle: Composition, Structure and Evolution, pp. 461–502, doi:10.1017/CBO9780511573101.013, 1998.

Lambeck, K., Yokoyama, Y., and Purcell, T.: Into and out of the Last Glacial Maximum: Sea-level change during Oxygen Isotope Stages 3 and 2, Quaternary Science Reviews, 21, 343–360, doi:10.1016/S0277-3791(01)00071-3, 2002.

Lambeck, K., Purcell, A., Johnston, P., Nakada, M., and Yokoyama, Y.: Water-load definition in the glacio-hydro-isostatic sea-level equation, Quaternary Science Reviews, 22, 309–318, doi:10.1016/S0277-3791(02)00142-7, 2003.

Larour, E., Seroussi, H., Morlighem, M., and Rignot, E.: Continental scale, high order, high spatial resolution, ice sheet modeling using the Ice Sheet System Model (ISSM), Journal of Geophysical Research: Earth Surface, 117, doi:10.1029/2011JF002140, 2012.

Le clec'h, S., Quiquet, A., Charbit, S., Dumas, C., Kageyama, M., and Ritz, C.: A rapidly converging initialisation method to simulate the present-day Greenland ice sheet using the GRISLI ice sheet model (version 1.3), Geoscientific Model Development, 12, 2481–2499, doi:10.5194/gmd-12-2481-2019, 2019.

Le Meur, E. and Huybrechts, P.: A comparison of different ways of dealing with isostasy: examples from modelling the Antarctic ice sheet during the last glacial cycle, Annals of Glaciology, 23, 309–317, doi:10.3189/S0260305500013586, 1996.

Leguy, G., Asay-Davis, X., and Lipscomb, W.: Parameterization of basal friction near grounding lines in a one-dimensional ice sheet model, The Cryosphere, 8, 1239–1259, doi:10.5194/tc-8-1239-2014, 2014.

Ma, Y., Gagliardini, O., Ritz, C., Gillet-Chaulet, F., Durand, G., and Montagnat, M.: Enhancement factors for grounded ice and ice shelves inferred from an anisotropic ice-flow model, Journal of Glaciology, 56, 805–812, doi:10.3189/002214310794457209, 2010.

MacAyeal, D. R.: Large-scale ice flow over a viscous basal sediment: Theory and application to ice stream B, Antarctica, Journal of Geophysical Research, 94, 4071–4087, doi:10.1029/JB094iB04p04071, 1989.

Mackintosh, A., Golledge, N., Domack, E., Dunbar, R., Leventer, A., White, D., Pollard, D., DeConto, R., Fink, D., Zwartz, D., Gore, D., and Lavoie, C.: Retreat of the East Antarctic ice sheet during the last glacial termination, Nature Geoscience, 4, 195, doi:10.1038/ngeo1061, 2011.

Mackintosh, A. N., Verleyen, E., O'Brien, P. E., White, D. A., Jones, R. S., McKay, R., Dunbar, R., Gore, D. B., Fink, D., Post, A. L., et al.: Retreat history of the East Antarctic ice sheet since the last glacial maximum, Quaternary Science Reviews, 100, 10–30, doi:10.1016/j.quascirev.2013.07.024, 2014.

https://doi.org/10.5194/tc-2020-28
Preprint. Discussion started: 10 March 2020

Maris, M., De Boer, B., Ligtenberg, S., Crucifix, M., Van De Berg, W., and Oerlemans, J.: Modelling the evolution of the Antarctic ice sheet since the last interglacial, The Cryosphere, 8, 1347–1360, doi:10.5194/tc-8-1347-2014, 2014.

Martin, M. A., Winkelmann, R., Haseloff, M., Albrecht, T., Bueler, E., Khroulev, C., and Levermann, A.: The Potsdam Parallel Ice Sheet Model (PISM-PIK)–Part 2: Dynamic equilibrium simulation of the Antarctic ice sheet, The Cryosphere, 5, 727–740, doi:10.5194/tc-5-727-2011, 2011.

Morlighem, M., Seroussi, H., Larour, E., and Rignot, E.: Inversion of basal friction in Antarctica using exact and incomplete adjoints of a higher-order model, Journal of Geophysical Research: Earth Surface, 118, 1746–1753, doi:10.1002/jgrf.20125, 2013.

Nakada, M., Kimura, R., Okuno, J., Moriwaki, K., Miura, H., and Maemoku, H.: Late Pleistocene and Holocene melting history of the Antarctic ice sheet derived from sea-level variations, Marine Geology, 167, 85–103, doi:10.1016/S0025-3227(00)00018-9, 2000.

Nicholls, R. J. and Cazenave, A.: Sea-level rise and its impact on coastal zones, Science, 328, 1517–1520, doi:10.1126/science.1185782, 2010.

Nowicki, S., Bindschadler, R. A., Abe-Ouchi, A., Aschwanden, A., Bueler, E., Choi, H., Fastook, J., Granzow, G., Greve, R., Gutowski, G., Herzfeld, U., Jackson, C., Johnson, J., Khroulev, C., Larour, E., Levermann, A., Lipscomb, W. H., Martin, M. A., Morlighem, M., Parizek, B. R., Pollard, D., Price, S. F., Ren, D., Rignot, E., Saito, F., Sato, T., Seddik, H., Seroussi, H., Takahashi, K., Walker, R., and Wang, W. L.: Insights into spatial sensitivities of ice mass response to environmental change from the SeaRISE ice sheet modeling project I: Antarctica, Journal of Geophysical Research: Earth Surface, 118, 1002–1024, doi:10.1002/jgrf.20081, 2013.

Pattyn, F.: Sea-level response to melting of Antarctic ice shelves on multi-centennial timescales with the fast Elementary Thermomechanical Ice Sheet model (f. ETISh v1. 0), The Cryosphere, 11, 1851, doi:10.5194/tc-11-1851-2017, 2017.

Pattyn, F.: The paradigm shift in Antarctic ice sheet modelling, Nature communications, 9, 2728, doi:10.1038/s41467-018-05003-z, 2018.

Pattyn, F., Perichon, L., Durand, G., Favier, L., Gagliardini, O., Hindmarsh, R. C., Zwinger, T., Albrecht, T., Cornford, S. L., Docquier, D., Fürst, J. J., Goldberg, D., Gudmundsson, G. H., Humbert, A., Hütten, M., Huybrechts, P., Jouvet, G., Kleiner, T., Larour, E., Martin, D., Morlighem, M., Payne, A. J., Pollard, D., Rückamp, M., Rybak, O., Seroussi, H., Thoma, M., and Wilkens, N.: Grounding-line migration in plan-view marine ice-sheet models: results of the ice2sea MISMIP3d intercomparison, Journal of Glaciology, 59, 410–422, doi:10.3189/2013JoG12J129, 2013.

Pattyn, F., Ritz, C., Hanna, E., Asay-Davis, X., DeConto, R., Durand, G., Favier, L., Fettweis, X., Goelzer, H., Golledge, N. R., Munneke, P. K., Lenaerts, J. T., Nowicki, S., Payne, A. J., Robinson, A., Seroussi, H., Trusel, L. D., and van den Broeke, M.: The Greenland and Antarctic ice sheets under 1.5° C global warming, Nature climate change, p. 1, doi:10.1038/s41558-018-0305-8, 2018.

Peltier, W. and Fairbanks, R. G.: Global glacial ice volume and Last Glacial Maximum duration from an extended Barbados sea level record, Quaternary Science Reviews, 25, 3322–3337, doi:10.1016/j.quascirev.2006.04.010, 2006.

Peltier, W., Argus, D., and Drummond, R.: Space geodesy constrains ice age terminal deglaciation: The global ICE-6G_C (VM5a) model., J. Geophys. Res. Solid Earth, 120, 450–487, doi:10.1002/2014JB011176, 2015.

Peltier, W., Argus, D., and Drummond, R.: Comment on "An Assessment of the ICE-6G_C (VM5a) Glacial Isostatic Adjustment Model" by Purcell et al., J. Geophys. Res. Solid Earth, 123, doi:10.1002/2016JB013844, 2018.

Peyaud, V., Ritz, C., and Krinner, G.: Modelling the Early Weichselian Eurasian Ice Sheets: role of ice shelves and influence of ice-dammed lakes, Climate of the Past Discussions, 3, 221–247, doi:10.5194/cp-3-375-2007, 2007.

Philippon, G., Ramstein, G., Charbit, S., Kageyama, M., Ritz, C., and Dumas, C.: Evolution of the Antarctic ice sheet throughout the last deglaciation: a study with a new coupled climate—north and south hemisphere ice sheet model, Earth and Planetary Science Letters, 248, 750–758, doi:10.1016/j.epsl.2006.06.017, 2006.

Pollard, D. and DeConto, R.: Description of a hybrid ice sheet-shelf model, and application to Antarctica, Geoscientific Model Development, 5, 1273–1295, doi:10.5194/gmd-5-1273-2012, 2012.

Quiquet, A., Dumas, C., Ritz, C., Peyaud, V., and Roche, D. M.: The GRISLI ice sheet model (version 2.0): calibration and validation for multi-millennial changes of the Antarctic ice sheet, Geoscientific Model Development, 11, 5003, doi:10.5194/gmd-11-5003-2018, 2018.

Reeh, N.: Parameterization of melt rate and surface temperature on the Greenland ice sheet, Journal of Geophysical Research: Solid Earth, 59, 113–128, doi:10.2312/polarforschung.59.3.113, 1989.

Reese, R., Albrecht, T., Mengel, M., Asay-Davis, X., and Winkelmann, R.: Antarctic sub-shelf melt rates via PICO, The Cryosphere, 12, 1969–1985, doi:10.5194/tc-12-1969-2018, 2018.

Rignot, E., Jacobs, S., Mouginot, J., and Scheuchl, B.: Ice-shelf melting around Antarctica, Science, 341, 266–270, doi:10.1126/science.1235798, 2013.

Ritz, C., Edwards, T. L., Durand, G., Payne, A. J., Peyaud, V., and Hindmarsh, R. C.: Potential sea-level rise from Antarctic ice-sheet instability constrained by observations, Nature, 528, 115, doi:10.1038/nature16147, 2015.

Robel, A. A., Seroussi, H., and Roe, G. H.: Marine ice sheet instability amplifies and skews uncertainty in projections of future sea-level rise, Proceedings of the National Academy of Sciences, 116, 14 887–14 892, doi:10.1073/pnas.1904822116, 2019.

Robinson, A., Calov, R., and Ganopolski, A.: Greenland ice sheet model parameters constrained using simulations of the Eemian Interglacial, Climate of the Past, 7, 381–396, doi:10.5194/cp-7-381-2011, 2011.

Robinson, A., Alvarez-Solas, J., Montoya, M., Goelzer, H., Greve, R., and Ritz, C.: Description and validation of the ice-sheet model Yelmo (version 1.0), Geosci. Model Dev. Discuss., doi:10.5194/gmd-2019-273, 2019.

Schaffer, J., Timmermann, R., Arndt, J. E., Kristensen, S. S., Mayer, C., Morlighem, M., and Steinhage, D.: A global, high-resolution data set of ice sheet topography, cavity geometry, and ocean bathymetry, Earth System Science Data, 8, 543, doi:10.5194/essd-8-543-2016, 2016.

Schoof, C.: The effect of cavitation on glacier sliding, Proceedings of the Royal Society A: Mathematical, Physical and Engineering Sciences, 461, 609–627, doi:10.1098/rspa.2004.1350, 2005.

Schoof, C.: A variational approach to ice stream flow, Journal of Fluid Mechanics, 556, 227–251, doi:10.1017/S0022112006009591, 2006.

Shapiro, N. M. and Ritzwoller, M. H.: Inferring surface heat flux distributions guided by a global seismic model: particular application to Antarctica, Earth and Planetary Science Letters, 223, 213–224, doi:10.1016/j.epsl.2004.04.011, 2004.

Simms, A. R., Lisiecki, L., Gebbie, G., Whitehouse, P. L., and Clark, J. F.: Balancing the last glacial maximum (LGM) sea-level budget, Quaternary Science Reviews, 205, 143–153, doi:10.1016/j.quascirev.2018.12.018, 2019.

Stolldorf, T., Schenke, H.-W., and Anderson, J. B.: LGM ice sheet extent in the Weddell Sea: evidence for diachronous behavior of Antarctic Ice Sheets, Quaternary Science Reviews, 48, 20–31, doi:10.1016/j.quascirev.2012.05.017, 2012.

Sutter, J., Gierz, P., Grosfeld, K., Thoma, M., and Lohmann, G.: Ocean temperature thresholds for Last Interglacial West Antarctic Ice Sheet collapse, Geophysical Research Letters, 43, 2675–2682, doi:10.1002/2016GL067818, 2016.

Sutter, J., Fischer, H., Grosfeld, K., Karlsson, N. B., Kleiner, T., Van Liefferinge, B., and Eisen, O.: Modelling the Antarctic Ice Sheet across the mid-Pleistocene transition–implications for Oldest Ice, The Cryosphere, 13, 2023–2041, doi:10.5194/tc-13-2023-2019, 2019.

Taylor, K. E., Stouffer, R. J., and Meehl, G. A.: An overview of CMIP5 and the experiment design, Bulletin of the American Meteorological Society, 93, 485–498, doi:10.1175/BAMS-D-11-00094.1, 2012.

The RAISED Consortium: A community-based geological reconstruction of Antarctic Ice Sheet deglaciation since the Last Glacial Maximum, Quaternary Science Reviews, 100, 1–9, doi:10.1016/j.quascirev.2014.06.025, 2014.

Van Wessem, J., Reijmer, C., Morlighem, M., Mouginot, J., Rignot, E., Medley, B., Joughin, I., Wouters, B., Depoorter, M., Bamber, J., Lenaerts, J., van der Berg, W., van den Broeke, M., and van Meijgaard, E.: Improved representation of East Antarctic surface mass balance in a regional atmospheric climate model, Cambridge University Press, 60, 761–770, doi:10.3189/2014JoG14J051, 2014.

Weertman, J.: On the sliding of glaciers, Journal of glaciology, 3, 33–38, doi:10.3189/S0022143000024709, 1957.

Whitehouse, P. L.: Glacial isostatic adjustment modelling: historical perspectives, recent advances, and future directions., Earth surface dynamics., 6, 401–429, doi:10.5194/esurf-6-401-2018, 2018.

Whitehouse, P. L., Bentley, M. J., and Le Brocq, A. M.: A deglacial model for Antarctica: geological constraints and glaciological modelling as a basis for a new model of Antarctic glacial isostatic adjustment, Quaternary Science Reviews, 32, 1–24, doi:10.1016/j.quascirev.2011.11.016, 2012a.

Whitehouse, P. L., Bentley, M. J., Milne, G. A., King, M. A., and Thomas, I. D.: A new glacial isostatic adjustment model for Antarctica: calibrated and tested using observations of relative sea-level change and present-day uplift rates, Geophysical Journal International, 190, 1464–1482, doi:10.1111/j.1365-246X.2012.05557.x, 2012b.

Whitehouse, P. L., Gomez, N., King, M. A., and Wiens, D. A.: Solid Earth change and the evolution of the Antarctic Ice Sheet, Nature communications, 10, 503, doi:10.1038/s41467-018-08068-y, 2019.

Winkelmann, R., Martin, M. A., Haseloff, M., Albrecht, T., Bueler, E., Khroulev, C., and Levermann, A.: The Potsdam parallel ice sheet model (PISM-PIK)–Part 1: Model description, The Cryosphere, 5, 715–726, doi:10.5194/tc-5-715-2011, 2011.

Zwally, H., Jay, M. B., Giovinetto, M. A. B., and Saba, J. L.: Antarctic and Greenland Drainage Systems, GSFC Cryospheric Sciences Laboratory, http://icesat4.gsfc.nasa.gov/cryo_data/ant_grn_drainage_systems.php, 2012.

https://doi.org/10.5194/tc-2020-28
Preprint. Discussion started: 10 March 2020

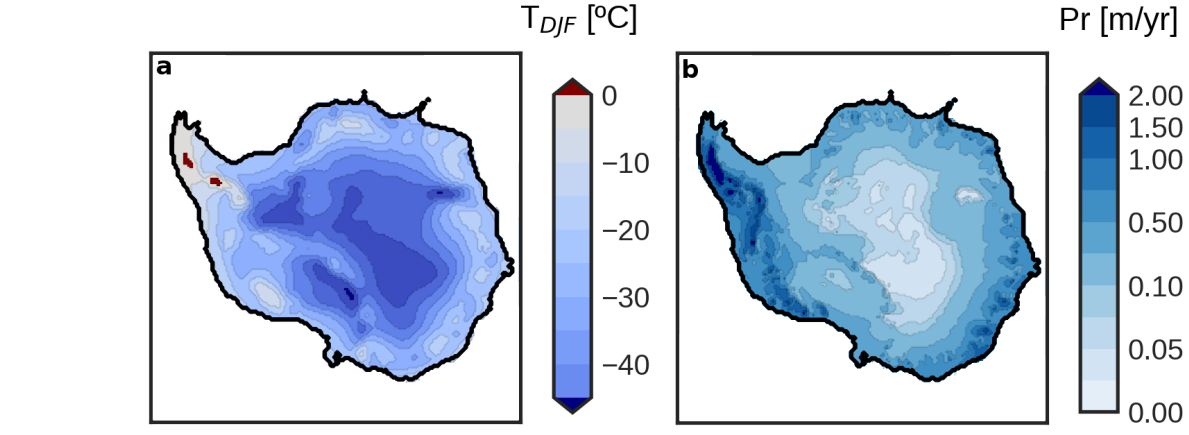

Figure 1. PMIP3 ensemble mean **(a)** surface summer temperature (in ºCelsius) and **(b)** annual precipitation (in $\mathrm{m\ yr^{-1}}$ water equivalent) at sea level. The thick black line shows the 2000 m-depth contour.

https://doi.org/10.5194/tc-2020-28
Preprint. Discussion started: 10 March 2020

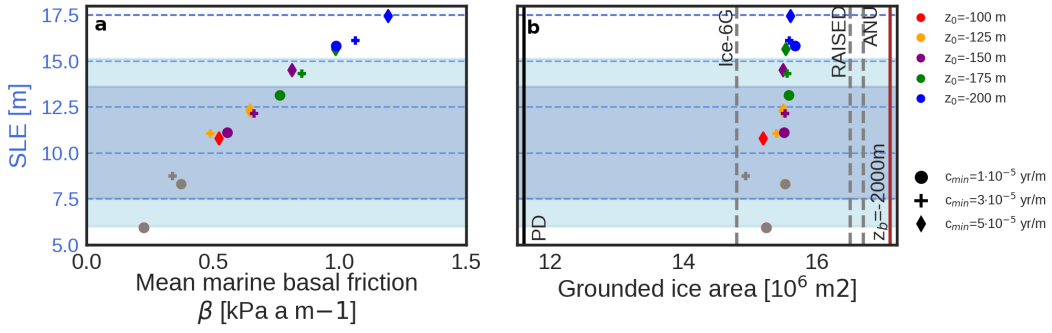

Figure 2. Scatter plot of the simulated LGM ice-volume anomaly (in msle, positive means ice-volume increase at the LGM) with respect to **(a)** the mean basal-drag coefficient and **(b)** the simulated grounded ice area, for the LGM simulations corresponding to different friction parameters. The dark blue horizontal area represents the SLE LGM estimates summarized by Simms et al. (2019) since 2010. The light blue area includes the uncertainties of the two extreme cases. The grey shaded vertical lines in **(b)** show the ice extension estimates from ICE-6G, The RAISED Consortium and the ANU reconstruction at the spatial resolution of our simulations (see main text). The black vertical line is the PD extension and the brown vertical line represents the computed ice area within the continental-shelf break defined as z_b>-2000 m. Grey-colour symbols represent simulations that did not produce a realistic PD state (see Supplementary Information).

https://doi.org/10.5194/tc-2020-28
Preprint. Discussion started: 10 March 2020

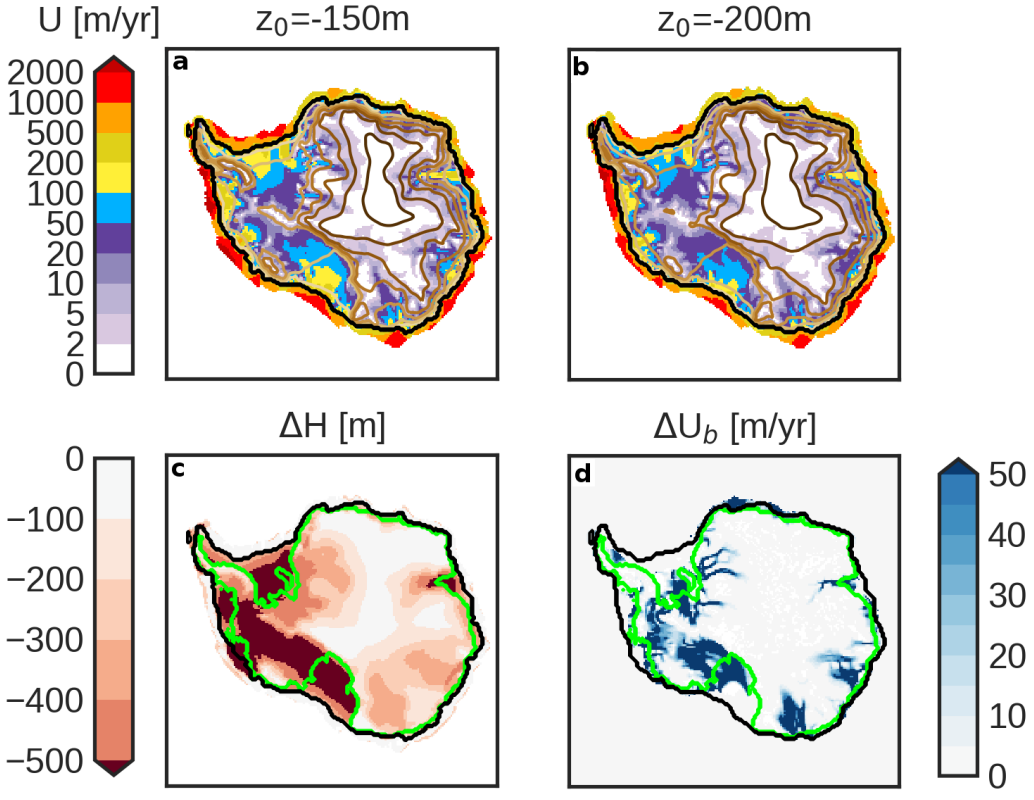

Figure 3. Simulated LGM surface elevation and velocity for c_{min}=1·10^{-5} yr m^{-1} for **(a)** z_0=-150 m and **(b)** z_0=-200 m; brown contours show surface elevation in 500 m intervals up to 3500 m above sea level. Difference in **(c)** ice thickness and **(d)** basal velocity between **(a)** and **(b)** (a minus b); the thick black line shows the grounding-line position of z_0=-200 m and the green line the PD grounding-line position.

https://doi.org/10.5194/tc-2020-28
Preprint. Discussion started: 10 March 2020

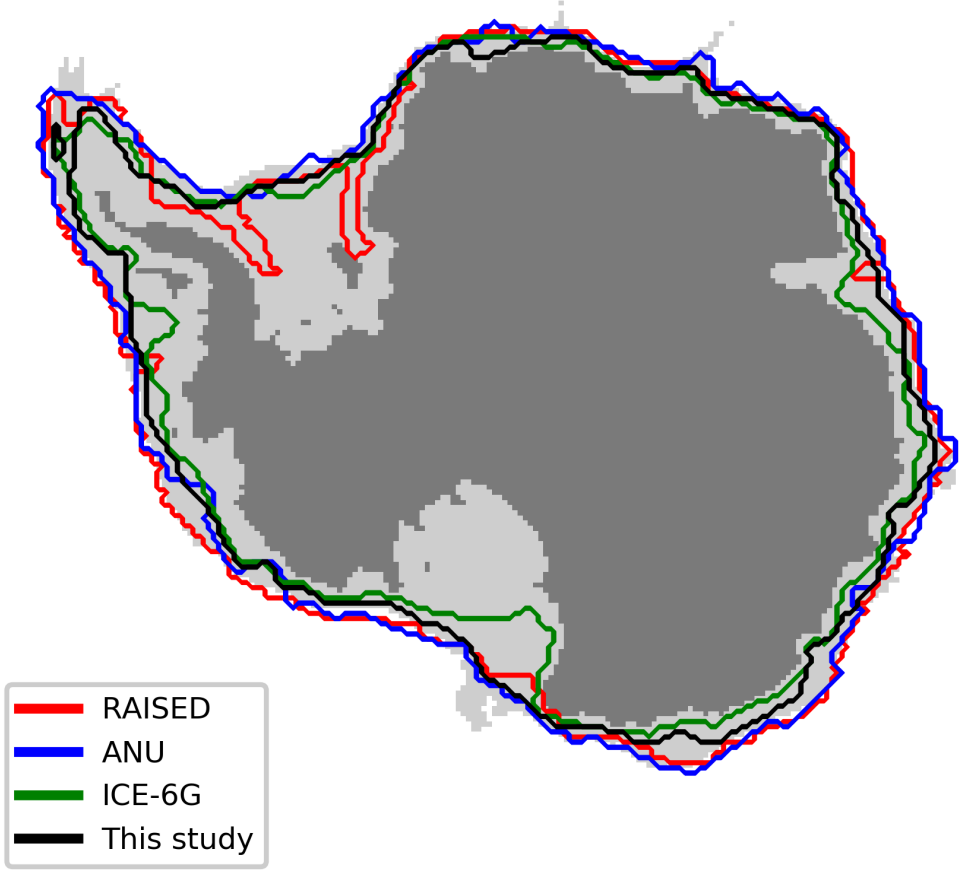

Figure 4. Grounded ice extensions reconstructions from RAISED Consortium in red; ANU in blue and ICE-6G in green. In black, the simulated ice extension in this study for z_0=-175 m and c_{min}= $1{\cdot}10^{-5}$ yr m^{-1}. The grey dark area shows the PD grounded ice. The area between the PD grounded area and the continental-shelf break (z_b<-2000 m) is shown in light grey.

https://doi.org/10.5194/tc-2020-28
Preprint. Discussion started: 10 March 2020

The Cryosphere Discussions
Open Access
EGU

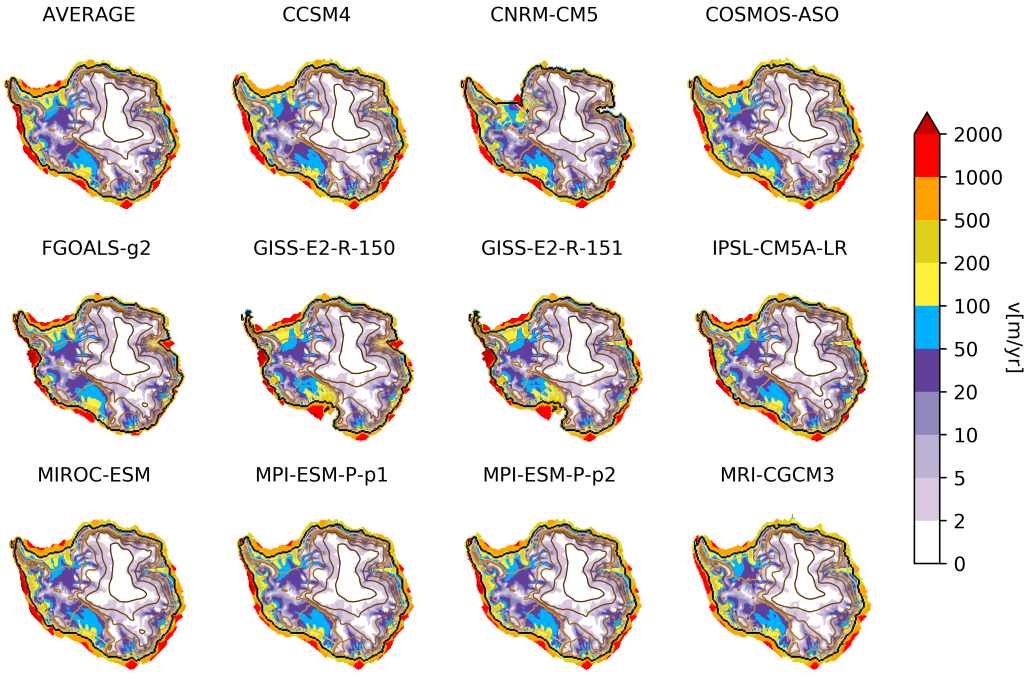

Figure 5. LGM AIS ice elevation (brown contours) and velocity (colors) simulated using the LGM minus PD anomalies of each of the PMIP3 ensemble-members as forcing (see main text). The thick black line shows the grounding-line position. The brown contours show surface elevation in 500 m intervals up to 3500 m above sea level.

https://doi.org/10.5194/tc-2020-28
Preprint. Discussion started: 10 March 2020

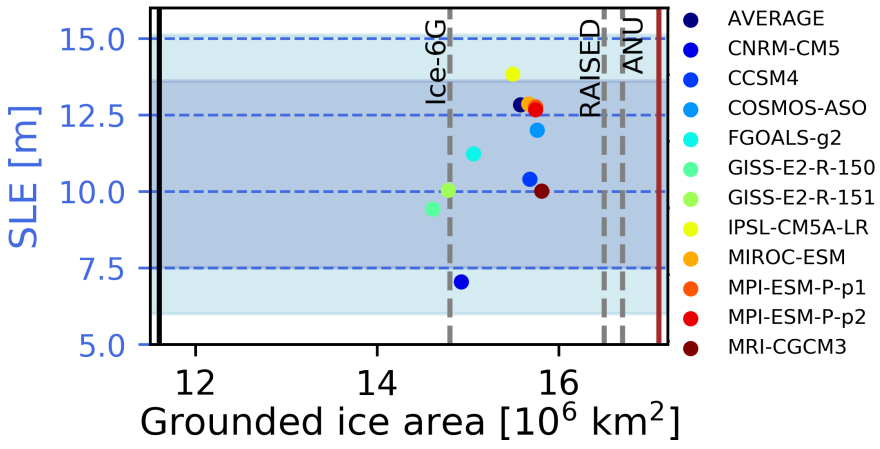

Figure 6. Scatter plot, as in Fig. 2, of the simulated LGM ice volume anomaly (SLE) against the grounded ice area for the PMIP3 ensemble and reference values of z_0=-175 m and c_{min}= $1{\cdot}10^{-5}$ yr m^{-1}.

https://doi.org/10.5194/tc-2020-28
Preprint. Discussion started: 10 March 2020

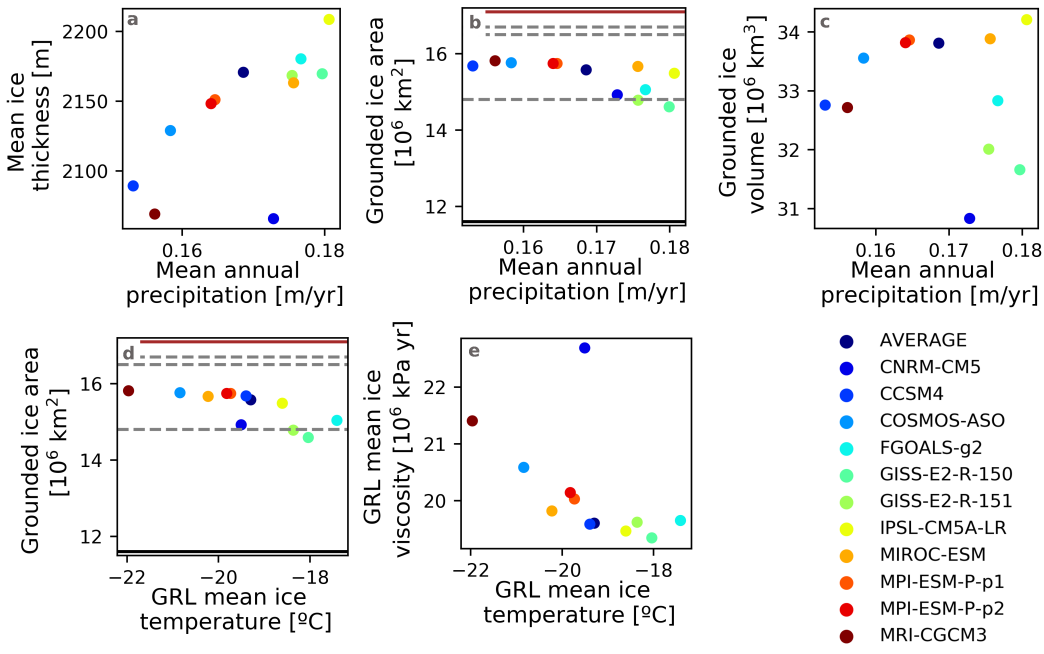

Figure 7. Scatter plots of **(a)** the mean ice thickness vs. the mean annual precipitation of the grounded grid points; **(b)** the grounded ice area vs. the mean annual precipitation of the grounded grid points; **(c)** the grounded ice volume vs. the mean annual precipitation of the grounded grid points; **(d)** the grounded ice area vs. the mean ice temperature at the grounding line; **(e)** the mean ice viscosity at the grounding line vs. the mean ice temperature at the grounding line. The horizontal lines in **(b)** and **(d)** represent the ice extensions described in Fig. 2.

https://doi.org/10.5194/tc-2020-28
Preprint. Discussion started: 10 March 2020

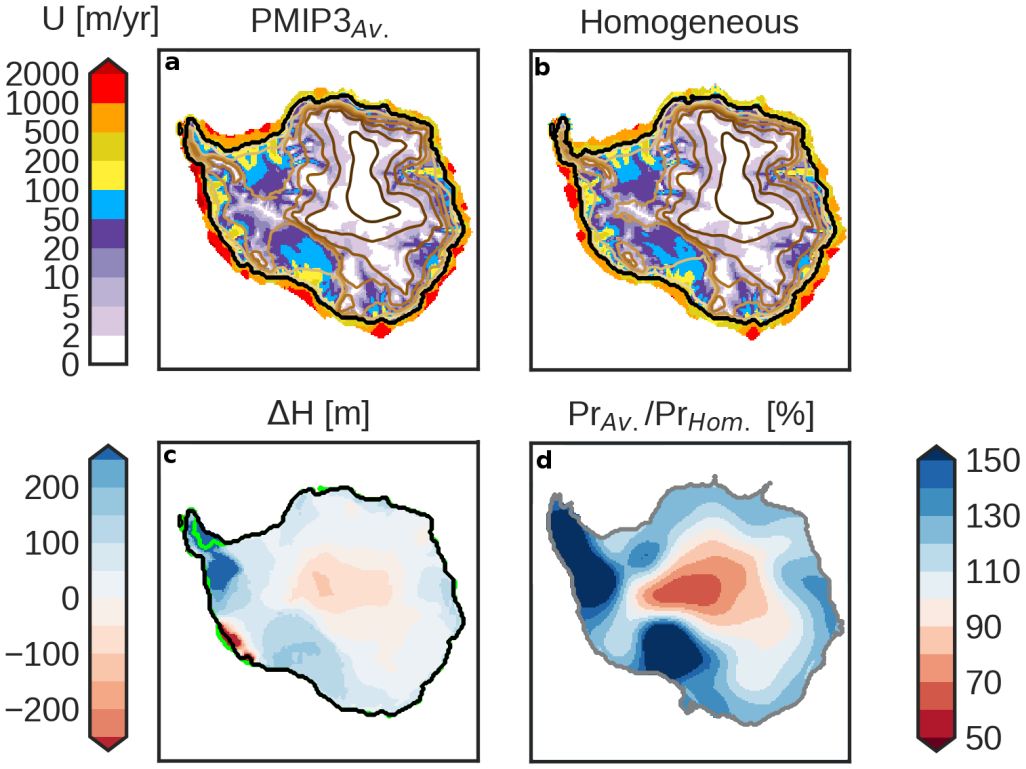

Figure 8. Simulated AIS LGM surface elevation and velocity when forcing with **(a)** the spatially homogeneous method and **(b)** the PMIP3 average snapshot with z_0=-175 m and c_{min}=1·10^{-5} yrm^{-1}. The thick black line shows the grounding-line position. The brown contours show surface elevation in 500 m intervals up to 3500 m above sea level. Panel **(c)** shows the ice thickness difference **(a)** minus **(b)**, where the thick green and black lines show the grounding-line position from the simulation with homogeneous and PMIP3 climatic forcing, respectively. Panel **(d)** shows the ratio of precipitation in the PMIP3 forced simulation to that of the homogeneous simulation and the grey line the continental-shelf break (z_b=-2000 m).